University of California

Los Angeles

Magnetic Field Feature Analysis of Smartphone Application Activities Using Android MI Sensors

A project submitted in partial satisfaction

of the requirements for the degree

Master of Science in Electrical Engineering

by

Hsin-Hao Chiang

2013

Abstract of the Project

Magnetic Field Feature Analysis of Smartphone Application Activities Using Android MI Sensors

by

Hsin-Hao Chiang

Master of Science in Electrical Engineering

University of California, Los Angeles, 2013

Professor Mani Srivastava, Chair

In this project, the magnetic field data of three axes are read by the magnetometer in an Android Smartphone and are recorded by an application then processed through MATLAB. Various denoising techniques and frequency domain analysis is implemented and two sets of experiment are designed by varying the direction, the phone activity, and the distance.

The first experiment is done in order to analyze the magnetic field feature generated by another smartphone, whereas the second experiment is to monitor the change of the magnetic field due to different activities running on the same phone. WiFi transmitting and music-playing activities are chosen for the test, and different characteristics of magnetic field features are discovered respectively.

The project of Hsin-Hao Chiang is approved.

Co-chair 1 name

Co-chair 2 name

Co-chair 3 name

Mani Srivastava, Committee Chair

University of California, Los Angeles

2013

Table of Contents

List of Figures

List of Tables

CHAPTER 1

Introduction

1.1 Magnetometer

The numbers and accuracy of sensors in Android Smartphone has increased tremendously since it has first been invented. Current Android API 17 indicates that nowadays a typical smartphone usually comes with sensors including accelerometer, gyroscope, proximity sensor, light sensor, and magnetometer, and some even have temperature and humidity sensors[1]. Data from single or multiple sensors provides information such as location, speed, orientation, or status of the phone or the user, which can further been processed for application usage, such as location-based services or gaming experience.

Among all the sensors, magnetometer has not widely been used or explored as a major sensor. In other industry magnetometer is already been used, such as vehicle detection[5]. Currently on Google Market most applications of magnetometer are for compass, metal detector, or simply magnetic field recorder. However, there are applications that use the magnetic data to achieve indoor navigation, such as IndoorAtlas ltd[6]. A team in Microsoft also do the indoor proximity detection by analyzing magnetic field characteristic, and they also claim that magnetometer has sharper boundaries, more consistent over time, and more resistant to interference than other techniques such as 802.15.4, Bluetooth Low Energy, or RFID in proximity detection[8].

Apple Inc. recently has patented a new method for triggering network device

discovery using magnetometer[4]. The speaker of the smartphone is connected to a magnetic field signature generator which generates a special pattern corresponding to the distinct ID of the phone. After the phone detects the specific magnetic feature, it then determines which type the object is and initiates the connection using Bluetooth, WiFi, or other connection protocols. The benefit for this scheme is lower energy consumption since magnetometer alone consumes less power than WiFi communication, and a new connection can be searched in magnetic domain while old connection remains active.

Since no phone has had the build-in magnetic feature generator yet, the purpose of the experiment is to determine if a phone can be discovered easily by its nature magnetic field, and what WiFi signals or speakers oscillation when music is played would influence the magnetic field value.

The smartphone used in the experiment is LG P999/G2X[7], and its magnetometer is AMI304, manufactured by Aichi Steel[3]. It has three magneto-impedance sensors aligned in 3 axes, and the sensitivity is 600 *LSB/Gauss*, or 0.167 uT.

Using the Android API SensorManager, one timestamp and three magnetic field data is fetched in every event. The fastest sampling frequency can be achieved by setting the delay to **SENSOR_DELAY_FASTEST**. The resulting actual sampling frequency tested on the device is 30 *Hz*.

1.2 Data Processing Method

An Android application is written to record and calculation the magnetic value of x, y, z, direction and the norm. The norm is calculated by the formula

$$B_n = \sqrt[2]{B_x^2 + B_y^2 + B_z^2} \tag{1.1}$$

The data is recorded in a *.csv* file. Further analysis is done by MATLAB

scripts. The sample input file is shown in Figure 1.1. 60 seconds of input data are recorded.

The norm value is then passed into a denoising filter using MATLAB script **cmddenoise()**. The filter performs an interval-dependent denoising of the signal, using a wavelet decomposition. Daubechies wavelet transform with level $N = 8$ is selected in this report, and the formula is shown in follow. Let

$$P(y) = \sum_{k=0}^{N-1} \binom{n}{k} y^k, \text{ where} \binom{n}{k} \text{denotes the binomial coefficients.} \tag{1.2}$$

Then

$$|m_0(\omega)|^2 = ((\cos^2(\frac{\omega}{2}))^N P(\sin^2(\frac{\omega}{2})), \text{ where } m_0(\omega) = \frac{1}{\sqrt{2}} \sum_{k=0}^{2N-1} h_k e^{-ik\omega} \tag{1.3}$$

The input and output of the filter is shown in Figure 1.2.

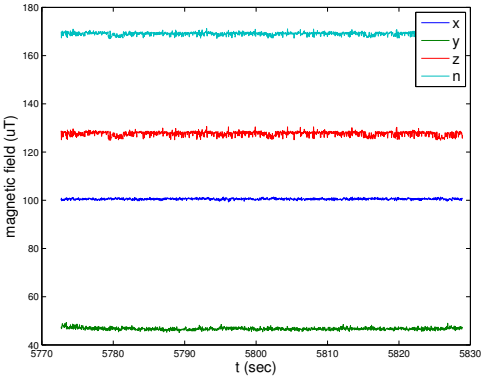

Figure 1.1: Sample input data.

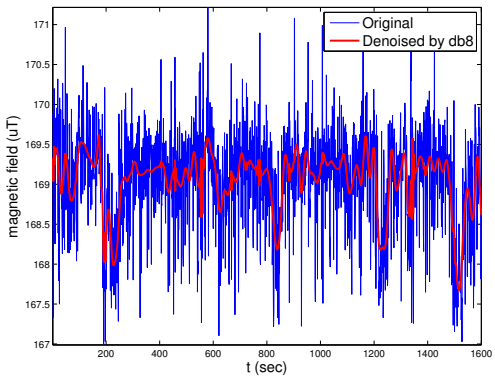

Figure 1.2: Denoised norm.

In order to analyze the frequency characteristics, **Short-Time Fourier Transform**(STFT) is implemented on the denoised signal. Setting *nfft* = 32, *noverlap* = 30, the output matrix is shown in Figure 1.3, and each column represents the instant frequency distribution from 0 to 32 *Hz* for the short time interval.

The final step is to observe the low and high frequency characteristics. We sum up the power ranging from 5 to 8 *Hz* to represent low frequency(**X**), and 15

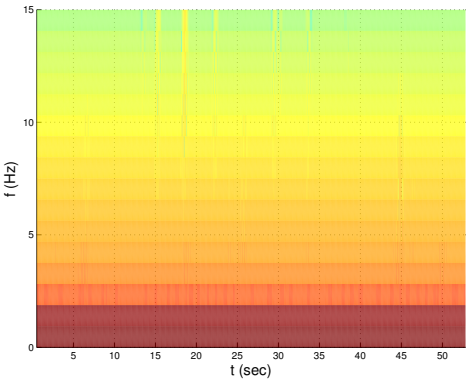

Figure 1.3: STFT output.

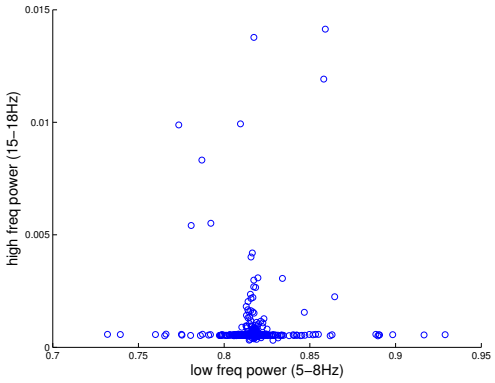

Figure 1.4: Scatter plot.

to 18 *Hz* for high frequency($\mathbf{Y}$). Then for each short time interval, we obtain a pair of power values ($\mathbf{X}$,$\mathbf{Y}$). By plotting $\mathbf{Y}$ vs $\mathbf{X}$ on a 2-D scatter plot, the pattern of the specific condition can be observed (see Figure 1.4), and different status can be further categorized.

CHAPTER 2

Experiment Result and Discussion

Two sets of experiments are done in this report. The first one is using an Android smartphone (phone A) to monitor the magnetic field generated by another Android smartphone (phone B). The second one is done using a single phone with different application running and recording at the same time.

2.1 Experiment I

2.1.1 Experiment Design

1. Phone A is always in airplane mode, and only the recording application is running.

2. Two phones always has same orientation, only change relative position.

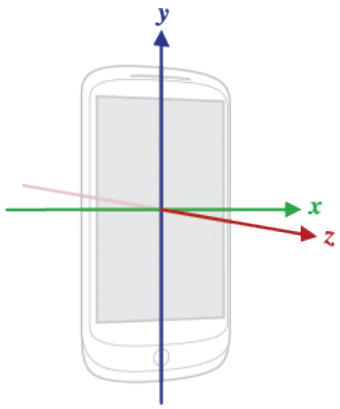

Figure 2.1: Phone orientation. [2]

3. The orientation of the phone is shown in Figure 2.1. Phone B is put in direction $+x$, $+y$, or $+z$ of phone A for testing.

4. Five different scenarios of phone B:

   (a) not present

   (b) airplane mode: idle

   (c) WiFi active: transmitting WiFi packets

   (d) music active: playing music in airplane mode

   (e) WiFi and music active: transmitting packets and playing music at the same time

5. Four different distances are tested: 0 ft, 0.5 ft, 1 ft, 1.5 ft.

2.1.2 Experimental Result

For mode a, X has avg = 394e-4, std = 112e-4, and Y has avg = 6.96e-4, std = 35e-4.

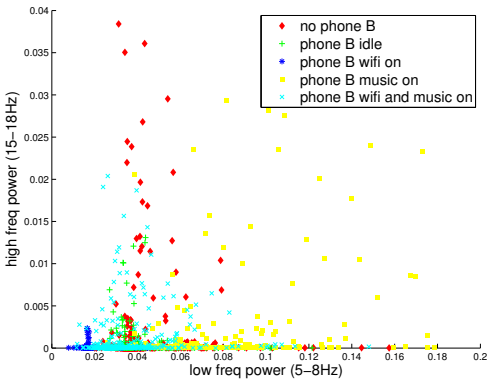

Figure 2.2: +x, 0 ft.

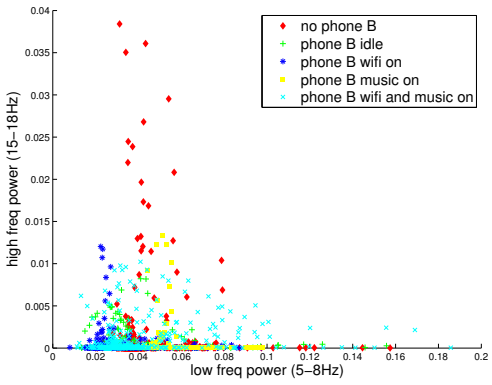

Figure 2.3: +x, 0.5 ft.

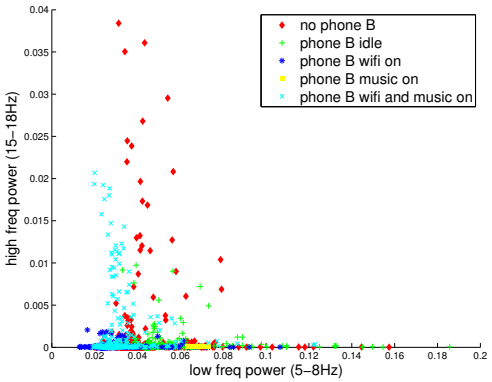

Figure 2.4: +x, 1.0 ft.

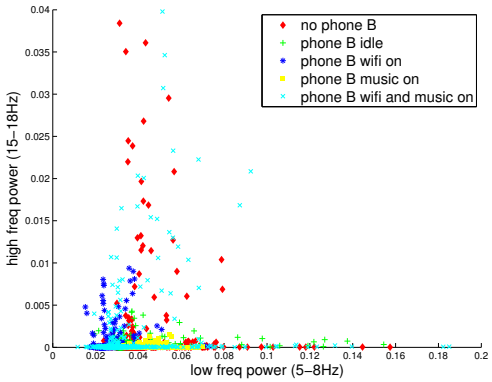

Figure 2.5: +x, 1.5 ft.

Table 2.1: x direction (in 1E-4)

	0 ft				0.5 ft			
	b	c	d	e	b	c	d	e
xavg	349.76	167.00	692.69	339.73	334.45	267.43	504.11	340.84
xstd	92.82	24.91	205.45	296.12	153.33	100.86	87.12	225.79
yavg	2.03	0.36	6.52	4.63	2.05	1.70	1.52	5.07
ystd	10.78	1.78	30.96	19.18	8.12	9.32	9.98	14.50
	1ft				1.5 ft			
	b	c	d	e	b	c	d	e
xavg	484.34	260.92	674.37	287.17	340.34	244.99	449.60	318.92
xstd	133.92	79.97	6.31	77.90	113.59	46.80	41.85	158.47
yavg	1.78	0.60	0.44	6.79	1.20	2.42	0.53	8.31
ystd	7.88	1.93	0.01	25.70	3.96	10.25	1.28	40.09

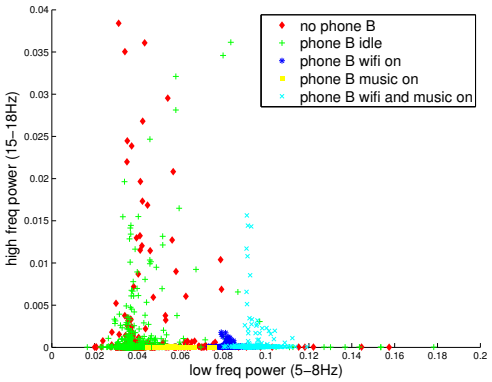

Figure 2.6: +y, 0 ft.

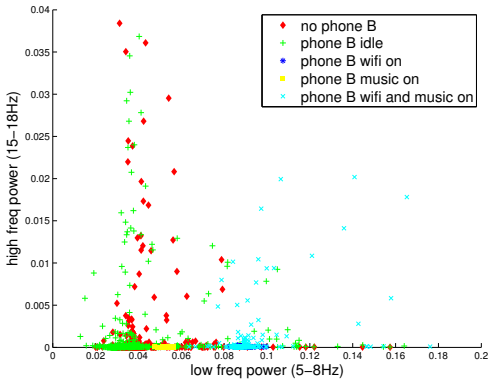

Figure 2.7: +y, 0.5 ft.

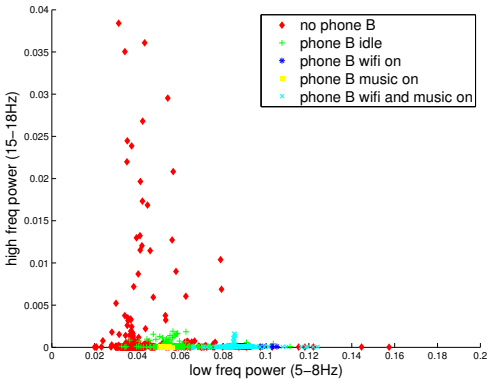

Figure 2.8: +y, 1.0 ft.

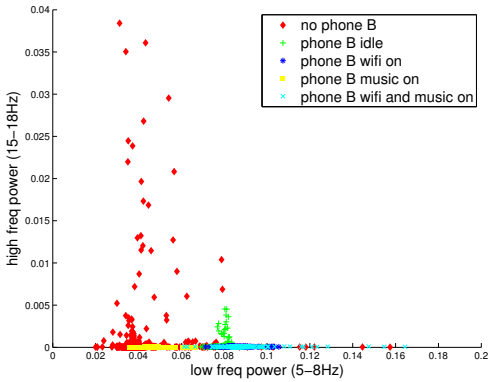

Figure 2.9: +y, 1.5 ft.

Table 2.2: y direction (in 1E-4)

	0 ft				0.5 ft			
	b	c	d	e	b	c	d	e
xavg	394.36	810.28	570.69	935.73	362.88	868.53	526.93	880.30
xstd	135.26	20.51	17.03	41.21	196.48	17.05	7.89	81.17
yavg	8.12	0.83	0.38	2.36	10.17	0.61	0.36	3.22
ystd	32.52	1.57	0.05	11.93	45.64	0.15	0.04	17.15
	1ft				1.5 ft			
	b	c	d	e	b	c	d	e
xavg	537.22	854.87	530.02	840.45	793.89	835.46	476.56	864.15
xstd	60.64	23.93	7.54	44.00	27.22	30.02	19.31	61.03
yavg	0.88	0.60	0.36	0.74	1.21	0.56	0.33	0.60
ystd	2.12	0.08	0.02	1.15	4.03	0.05	0.04	0.09

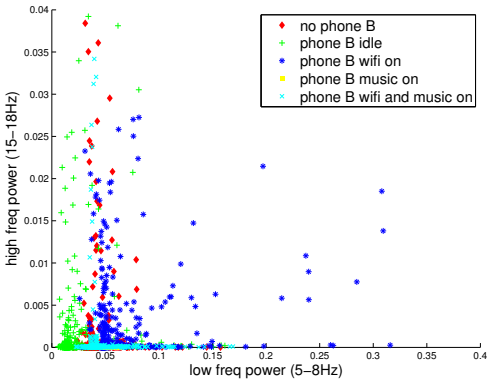

Figure 2.10: +z, 0 ft.

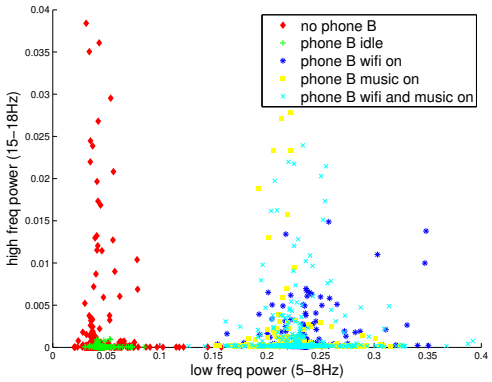

Figure 2.11: +z, 0.5 ft.

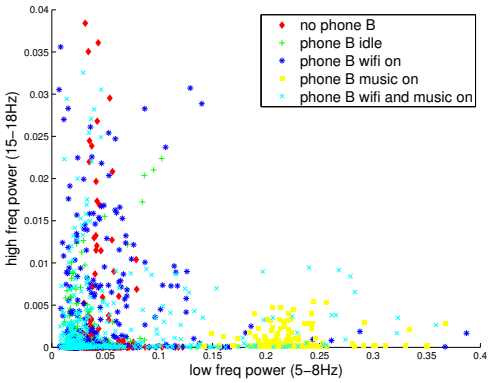

Figure 2.12: +z, 1.0 ft.

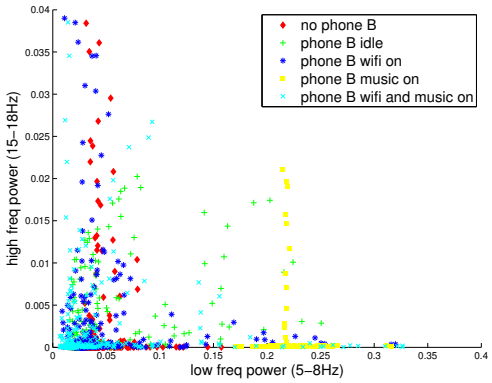

Figure 2.13: +z, 1.5 ft.

Table 2.3: z direction (in 1E-4)

	0 ft				0.5 ft			
	b	c	d	e	b	c	d	e
xavg	202.22	561.60	451.79	418.50	460.11	2443.46	2232.22	2389.61
xstd	180.54	303.37	19.90	140.76	39.68	132.39	158.33	139.29
yavg	8.64	12.45	0.31	3.32	0.50	3.02	4.45	3.21
ystd	38.44	37.88	0.03	25.61	0.95	7.38	21.22	7.94
	1ft				1.5 ft			
	b	c	d	e	b	c	d	e
xavg	206.94	350.28	2173.10	374.39	302.67	339.17	2180.33	258.46
xstd	113.19	458.52	164.94	474.71	261.79	285.27	81.87	390.34
yavg	5.13	21.47	2.94	12.81	8.47	11.10	3.07	9.50
ystd	21.17	73.66	6.15	37.89	28.77	48.02	15.59	43.74

2.1.3 Discussion

1. In general

    - When phone B is placed by phone A, Y is suppressed, ie. high frequency power is lowered.
    - The power does not decrease monotonically when the distance increases. It is interesting that there exist some magnetic field peaks in some direction.

2. In terms of direction and distance:

    - In direction $+x$, two phones are placed side by side, and therefore all scenarios overlap each other and are not easy to be categorized. However, it is still clear that mode (a) and mode (b) have similar **X** and in mode (c) **X** remains in low power (around 0.02). Increase the distance only impacts mode(d).
    - In direction $+y$, mode (e) is most distinguished from others. **Y** in mode (d) remains low and all Ys become zero when distance increases.
    - In direction $+z$, phone B is on top of phone A, it has largest impact to magnetic field when transmitting WiFi packets. However, the result shows that the influence is not directly inverse relative to the distance. mode (d) can barely observed when 0 ft, but can be observed in larger distance, and its **X** even converge at 1.5 ft. It implies the magnetic field of a smartphone has special pattern. Mode (c)(d)(e) all have larger **X** at 0.5 ft confirms this result.

3. In terms of scenario:

    - In mode (a)(red cursor), phone A only records the weak magnetic field, so **Y**is random and as large as 0.04 but **X** is stable within 0.03 and 0.05

- In mode (b)(green cursor), **Y**is lower than (a), and **X** is more concentrated. It is because phone B implies a small but constant magnetic field on phone A, so the STFT result would be more static.
- In mode (c)(blue cursor), the WiFi module of phone B is constantly transmitting packets and the magnetic is varying largely due to the change of electromagnetic wave. Consequently, **X** and **Y** are both random.
- In mode (d)(yellow cursor), phone B plays a segment of music in airplane mode, so the magnetic field is mostly influenced by the electromagnet in the speaker. The resulting **Y**is relatively low (below 0.02), and **X** is static around 0.05
- In mode (e)(cyan cursor), both WiFi transmission and music play are active, As a result, the scatter plot is the superposition of mode (c) and (d).

2.2 Experiment II

2.2.1 Experiment Design

The second experiment is done by monitoring the change of magnetic field when the phone itself is running different activities. Similar activities are chosen: WiFi packet transmission and music play. Phone call activity is also added.

2.2.2 Experimental Result

The scatter plot (Figure 2.14) shows that the phone call activity has large influence on magnetic field compared to other activities. For other activities, the zoomed plot (Figure 2.15) shows that it can easily detect its WiFi activity due to the larger variance of **X** than idle, but music play is rather difficult to detect.

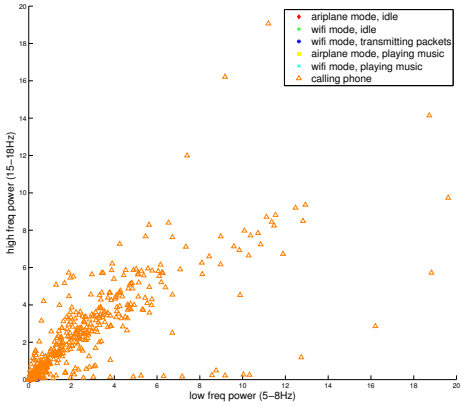

Figure 2.14: Experiment II.

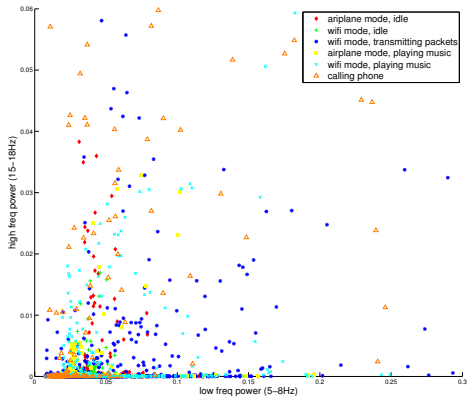

Figure 2.15: Experiment II zoom in.

Table 2.4: Experiment II (in 1E-4)

	a	b	c	d	e	f
xavg	393.73	410.92	542.81	304.08	383.95	16360.75
xstd	111.83	83.99	517.58	154.60	335.48	27790.66
yavg	6.93	2.42	19.83	4.09	21.87	14677.55
ystd	35.24	13.56	69.50	25.32	116.32	24170.47

CHAPTER 3

Conclusion

3.1 Summary

1. The magnetic field characteristic of an Android smartphone varies significantly depending on the status of the phone, the modules which are active, and the applications which are running. Through frequency analysis using STFT, different status can be categorized statistically. The study implies that the magnetometer of the smartphone can be used not only as a compass, but more as a detector or tracker of surrounding environment, or even the activities of itself.

2. Phone call generates large magnetic field and can be easily detected. It is possibly due to the mobile network and depends on the signal strength. s

3. It is shown that the magnetic field would vary largely when WiFi packet transmission is active. Further investigation could be done on differentiating different type of WiFi activities, such as streaming video, file download, or social networking update.

4. It is proved that playing music is proved to be affective the magnetic field. Apple Inc. proposed the method to emit magnetic field spike using the speaker should be feasible, but it should not generate unwanted sound at the same time.

5. Different distances and phone orientations will result in different magnetic feature. An omni-directional detecting algorithm is needed in order to provide

more reliable categorization.

6. It could be a privacy issue since the magnetic field data can be easily captured by third-party. It is interesting to study if any shielding can reduce such effect.

3.2 Future Work

1. The sampling period of the data provided by Android sensor API is not static, and it depends on the priority of the application process and the loading of the OS. In this report it is assumed that the sampling interval remains stable in a short time period. The background running applications of the recording smartphone is reduced to as few as possible, but sometimes jitter still happens. It could be done by directly accessing the magnetometer data, but a general user application should only use OS-provided API.

2. The change of DC or very low frequency value is not discussed in this report. It is because sometimes significant changing of the magnetic field will cause the magnetometer to become a very large value and lose track of actual DC value. Only after the user moves or shakes the phone, it will recalibrate and go back to the previous value. Apparently the large change of the magnetic field indicates the change of the state, so if taking it into consideration, the categorizing process may be more accurate.

3. Apple Inc. proposed a magnetic field signature generator coupled with the speaker in order to generate the magnetic spike. It is interesting to study which sound could generate such effect so that no additional hardware would be needed.

4. The data is recorded and are processed off-line using MATALB. It can be done by doing real-time calculation within the application on Android OS. However, the computation loading may affect the sampling period as discussed in 1.

Multicore processors or carefully-designed software can be implemented

5. In Experiment II it is shown that the WiFi activity of itself will impact on the detection of magnetometer. When a smartphone is in daily usage, i.e. mobile network and WiFi active, the result can be anticipated to be more noisy and harder to distinguish.

References

[1] Anrdoid API-Sensor. http://developer.android.com/reference/android/hardware/sensor.html.

[2] Android API-SensorEvent. http://developer.android.com/reference/android/hardware/sensorev

[3] Ami304 datasheet. http://www.aichi-mi.com/3_products/b9110329ami304e.pdf.

[4] Apple Inc. http://www.google.com/patents/us8290434.

[5] Yuqiao Shi Jinhui Lan. Vehicle detection and recognition based on a mems magnetic sensor. *IEEE International Conference on Nano/Micro Engineered and Molecular Systems*, January 2009.

[6] IndoorAtlas ltd. http://www.indooratlas.com/.

[7] G2X manual. http://extabit.com/file/28e6i5q276zn6/lg_p999_p999dw_t-mobile_g2x_service_manual.rar.

[8] Kaifei Chen Ben Zhang Jeff Hsu Jie Liu Bin Cao Xiaofan Jiang, Chieh-Jan Mike Liang and Feng Zhao. Design and evaluation of a wireless magnetic-based proximity detection platform for indoor applications. *IPSN*, April 2012.